

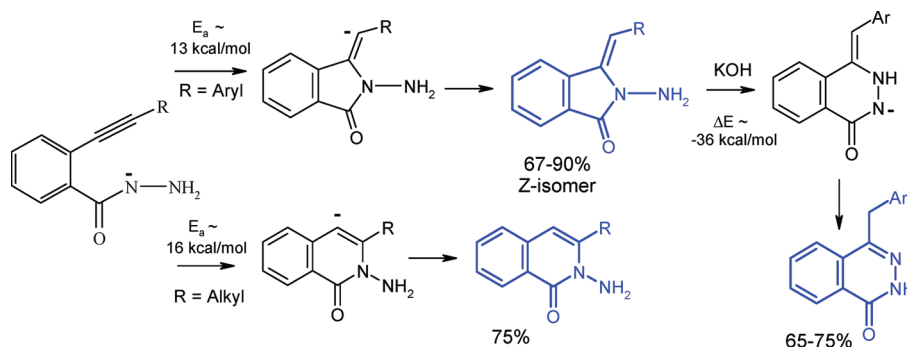
## Tuning Selectivity of Anionic Cyclizations: Competition between 5-Exo and 6-Endo-Dig Closures of Hydrazides of *o*-Acetylenyl Benzoic Acids and Based-Catalyzed Fragmentation/Recyclization of the Initial 5-Exo-Dig Products

Sergey F. Vasilevsky,<sup>\*,†</sup> Tat'yana F. Mikhailovskaya,<sup>†</sup> Victor I. Mamatyuk,<sup>‡</sup>  
 Georgy E. Salnikov,<sup>‡</sup> Georgy A. Bogdanchikov,<sup>†,§</sup> Mariappan Manoharan,<sup>⊥</sup> and  
 Igor V. Alabugin<sup>\*,¶</sup>

<sup>†</sup>Institute of Chemical Kinetics and Combustion, Novosibirsk 630090, Russian Federation, <sup>‡</sup>N. N. Vorozhtsov Novosibirsk Institute of Organic Chemistry, Siberian Branch of the Russian Academy of Sciences, 630090, Novosibirsk, Russian Federation, <sup>§</sup>Institute of Computational Mathematics and Mathematical Geophysics, Novosibirsk 630090, Russian Federation, <sup>⊥</sup>School of Science, Engineering and Mathematics, Bethune-Cookman University, Daytona Beach, Florida 32114, and <sup>¶</sup>Department of Chemistry and Biochemistry, Florida State University, Tallahassee, Florida 32306

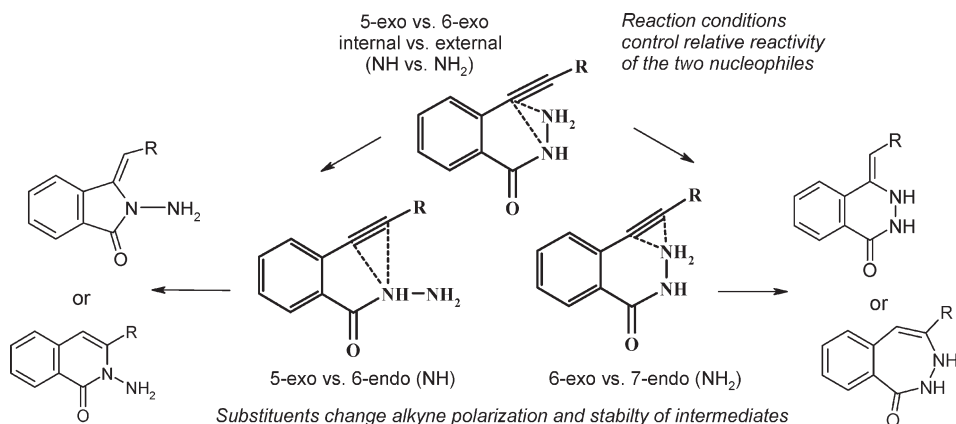
vasilev@kinetics.nsc.ru; alabugin@chem.fsu.edu

Received July 17, 2009



Depending on the reaction conditions and the nature of substituents at the triple bond, anionic cyclizations of hydrazides of *o*-acetylenyl benzoic acids can be selectively directed along three alternative paths, each of which provides efficient access to a different class of nitrogen heterocycles. The competition between 5-exo and 6-endo cyclizations of the “internal” nitrogen nucleophile is controlled by the nature of alkyne substituents under the kinetic control conditions. In the presence of KOH, the initially formed 5-exo products undergo a new rearrangement that involves a ring-opening followed by recyclization to the formal 6-exo-products and rendered irreversible by a prototropic isomerization. DFT computations provide insight into the nature of factors controlling relative rates of 5-exo, 6-endo, and 6-exo cyclization paths, ascertain the feasibility of direct 6-exo closure and relative stability for the anionic precursor for this process, provide, for the first time, the benchmark data for several classes of anionic nitrogen cyclizations, and dissect stereoelectronic effects controlling relative stability of cyclic anionic intermediates and influencing reaction stereoselectivity. We show that the stability gain due transformation of a weak  $\pi$ -bond into a stronger  $\sigma$ -bond (the usual driving force for the cyclizations of alkynes) is offset in this case by the transformation of a stable nitrogen anion into an inherently less stable carbanionic center. As a result, the cyclizations are much more sensitive to external conditions and substituents than similar cyclizations of neutral species. However, the exothermicity of such anionic cyclizations is increased dramatically upon prototropic isomerization of the initially formed carbanions into the more stable N-anions. Such tautomerizations are likely to play the key role in driving such cyclizations to completion but may also prevent future applications of such processes as the first step in domino cyclization processes.

## SCHEME 1. Two Levels of Selectivity in Cyclizations of Alkynes Promoted by Bifunctional Reagents



## Introduction

Diverse chemistry and broad synthetic potential of polyfunctional arylacetylenes continues to draw the attention of organic and medicinal chemists.<sup>1</sup> When the functional groups are positioned in the direct vicinity of the alkyne moiety, such compounds serve as convenient building blocks for the preparation of condensed heterocycles with a large scope of biological activity. From the fundamental perspective, these molecules lend themselves for investigation of internal and external factors controlling cyclization processes (structure of substrate, electronic and spatial parameters, etc.)<sup>2,3</sup> as well as convenient structural platforms for the design of molecular systems with controlled reactivity.<sup>4</sup>

Cyclizations of hydrazides of *o*-acetylenyl pyrazolcarboxylic acids illustrate how the multifunctional character of these substrates such as the different reactivity of the  $\alpha$ - and  $\beta$ -atoms in the triple bond and two nucleophilic centers (“amine” and “amide” nitrogen atoms) in the hydrazide moiety can be translated in the multichannel character of their transformations.<sup>5,6,7</sup> In particular, attack of the internal (“amide”) nitrogen at the triple bond can lead to

either 5-exo-dig (“internal carbon attack”) or 6-endo-dig (“external carbon attack”) cyclizations (Scheme 1). In a similar manner, external (“amine”) nitrogen can participate in either 6-exo- or 7-endo-dig cyclizations. All of these cyclizations are allowed by the Baldwin rules,<sup>8</sup> and thus the competition between these processes needs to be understood and controlled for achieving high selectivity in practical applications.<sup>9</sup>

In addition, the competition between the four possible cyclization routes should provide valuable fundamental information about the relative efficiency of these common transformations of anionic nitrogen nucleophiles. Current literature regarding cyclizations of *vic*-acetylenylbenzoic acid is limited to only two examples,<sup>10,11</sup> and thus cannot paint the full picture of basic heterocyclization trends.

Our recent communication reported cyclizations of two hydrazides of *o*-acetylenyl benzoic acids bearing *p*-methoxyphenyl and 1,5-dimethylpyrazol-4-yl substituents at the alkyne moiety (Scheme 2). Although we observed the 5-exo-dig cyclization with the formation of (*Z*)-2-amino-3-(4-methoxybenzylidene)isoindolin-1-one (67%) in the first case, cyclization of the pyrazolyl derivative unexpectedly yielded the product of a formal 6-exo-dig cyclization, 4-((1,5-dimethyl-1*H*-pyrazol-4-yl)methyl)phtalazin-1(2*H*)-one, in 70% yield.<sup>12</sup>

According to our earlier observations,<sup>10,11</sup> formation of the diazinone ring for the related compounds occurred only in the presence of CuCl and only under the neutral conditions where the “amine” nitrogen atom behaves as a stronger nucleophile than the “amide” nitrogen atom. This transformation can be formally described as the result of 6-exo attack at the  $\alpha$ -acetylenic carbon by the “amine” nitrogen with the following prototropic isomerization. This process would be unusual because, in the presence of KOH, the “amine” nitrogen is a weaker nucleophile than the *N*-anion formed via deprotonation at the “amide” nitrogen, and thus direct participation of the “amine” nitrogen in the diazinone formation is unlikely. An alternative scenario that includes

(1) *Acetylene Chemistry: Chemistry, Biology and Material Science*; Diederich, F.; Stang, P. J.; Tykwinski, R. R., Eds.; Wiley-VCH: Weinheim, Germany, 2005.

(2) Sakamoto, T.; Kondo, Y.; Yamanaka, M. *Heterocycles* **1988**, *27*, 2225.

(3) Vasilevsky, S. F.; Tretyakov, E. V.; Elguero, J. *Adv. Heterocycl. Chem.* **2002**, *82*, 1. Vasilevsky, S. F.; Baranov, D. S.; Mamatyuk, V. I.; Gatilov, Y. V.; Alabugin, I. V. *J. Org. Chem.* **2009**, *74*, 6143.

(4) Zeidan, T. A.; Manoharan, M.; Alabugin, I. V. *J. Org. Chem.* **2006**, *71*, 954. Zeidan, T.; Kovalenko, S. V.; Manoharan, M.; Alabugin, I. V. *J. Org. Chem.* **2006**, *71*, 962. Alabugin, I. V.; Manoharan, M. *J. Phys. Chem. A* **2003**, *107*, 3363. Alabugin, I. V.; Manoharan, M.; Kovalenko, S. V. *Org. Lett.* **2002**, *4*, 1119. Alabugin, I. V.; Gilmore, K.; Patil, S.; Manoharan, M.; Kovalenko, S. V.; Clark, R. J.; Ghiviriga, I. *J. Am. Chem. Soc.* **2008**, *30*, 11535.

(5) Vasilevsky, S. F.; Mshvidobadze, E. V.; Elguero, J. *J. Heterocycl. Chem.* **2002**, *39*, 1229.

(6) Vasilevsky, S. F.; Mshvidobadze, E. V.; Mamatyuk, V. I.; Romanenko, G. V.; Elguero, J. *Tetrahedron. Lett.* **2005**, *46*, 4457.

(7) For a recent interesting example of multifunctional reactivity of hydrazides, see: Roveda, J.-G.; Clavette, C.; Hunt, A. D.; Gorelsky, S. I.; Whipp, C. J.; Beauchemin, A. M. *J. Am. Chem. Soc.*, **2009**, *131*, 8740.

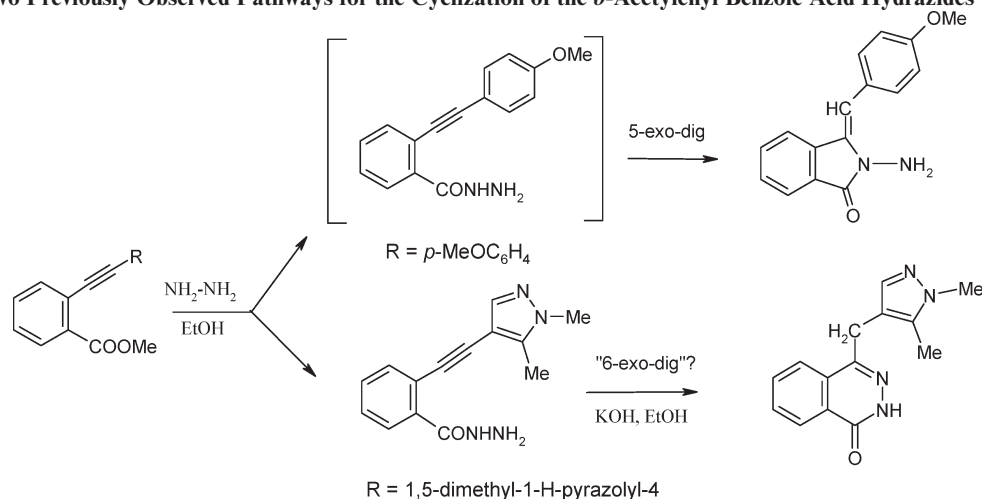
(8) Baldwin, J. E. *J. Chem. Soc., Chem. Commun.* **1976**, 734. See also: Beckwith, A. L. J.; Easton, C. J.; Serelis, A. K. *J. Chem. Soc., Chem. Commun.* **1980**, 482-483. For a useful mnemonics for Baldwin rules, see: Juaristi, E.; Cuevas, G. *Rev. Soc. Quim. Mex.* **1992**, *36*, 48.

(9) For the general analysis of factors responsible for a similar 5-exo-/6-endo competition in radical cyclizations, see: Alabugin I. V.; Manoharan, M. *J. Am. Chem. Soc.* **2005**, *127*, 12583.

(10) Vasilevsky, S. F.; Pozdnyakov, A. V.; Shvartsberg, M. S. *Izv. Akad. Nauk SSSR, Ser. Khim.* **1985**, *6*, 1367.

(11) Vasilevsky, S. F.; Pozdnyakov, A. V.; Shvartsberg, M. S. *Izv. Sib. Otd. Akad. Nauk SSSR, Ser. Khim.* **1985**, *5*, 83.

(12) Vasilevsky, S. F.; Mikhailovskaya, T. F. *Chem. Heterocycl. Compd.* **2009**, *1*, 67.

SCHEME 2. Two Previously Observed Pathways for the Cyclization of the *o*-Acetylenyl Benzoic Acid Hydrazides

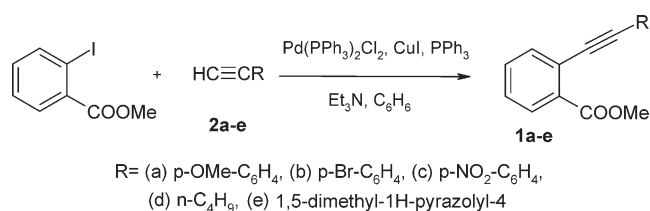
a rearrangement of an initially formed product seems more plausible than the direct 6-exo closure.

All of the above, along with the large effect of substituents on the observed selectivity,<sup>6</sup> motivated us to carry out a systematic study of such cyclizations using a broader selection of substituents. This study should also be of practical value because the cyclization pathways will produce medicinally interesting compounds with a promising spectrum of biological activity. For example, 4-hetaryl-1(2*H*)-phthalazinones proved to be effective antiasthmatic and bronchodilating agents<sup>13,14</sup> whereas benzopyridazinones display promising properties as melanin-concentrating hormone antagonists for treatment of anorexia, obesity, and diabetes.<sup>15</sup>

## Results and Discussion

Sonogashira cross-coupling of terminal alkynes with appropriately substituted aromatic halides continues to be a highly convenient method for the preparation of aryl- and hetaryl-acetylenes with ortho-substituents.<sup>16,17</sup> Thus, the starting materials for this study—esters of *o*-acetylenylbenzoic acids **1a–e**—were prepared through the reaction of the methyl ester of *o*-iodobenzoic acid with the appropriate alkynes **2a–e** under Cu–Pd catalysis in the Pd(PPh<sub>3</sub>)<sub>2</sub>Cl<sub>2</sub>/CuI/NEt<sub>3</sub> system in 67–97% yields (Scheme 3).

Heating ethynylbenzoates **1a–d** with hydrazine hydrate in ethanol led directly to the cyclization products **3a–c** (67–90%) without the intermediate accumulation of hydrazides **4a–c** (Scheme 4). Only in the case of the *n*-butyl

SCHEME 3. Cross-Coupling of Methyl Ester of *o*-Iodobenzoic Acid with Terminal Alkynes

substituent could the intermediate acetylenyl hydrazide **4d** be isolated (in 80% yield). Interestingly, the yield of the 5-exo product increased for the acceptor aryl substituents in accord with the buildup of negative charge at the benzylic carbon in the TS for the ring closure step.

Although chemical shifts of the endo- and exo-methyne hydrogens in the 1D <sup>1</sup>H NMR spectra of the  $\gamma$ - and  $\delta$ -*N*-aminolactams are similar, the isoindolinone structure of the products can be unambiguously determined by using 2D <sup>1</sup>H–<sup>1</sup>H correlations with double quantum filter (COSYDQF), one bond (HSQC), and long-range (HMBC) inverse <sup>13</sup>C–<sup>1</sup>H correlations. As an example, the signal assignments for the methoxy-derivative **3a** are given in the SI. The 5- and 6-membered condensed cycles can also be conveniently distinguished from the observed differences in the IR frequencies for the CO groups. The increase in strain upon the transition from a six- to a five-membered cycle caused increase of  $\nu(\text{CO})$  by 30–35 cm<sup>−1</sup>.<sup>18</sup> It is known that, in  $\delta$ -lactams, the valence stretch frequency of the CO-group,  $\nu(\text{CO})$ , is ca. 1660–1680 cm<sup>−1</sup>, whereas in  $\gamma$ -lactams this frequency exceeds 1695–1700 cm<sup>−1</sup>. The observed  $\nu(\text{CO})$  value of 1706–1716 cm<sup>−1</sup> in isolated lactams **3a–c** is fully consistent with the assigned  $\gamma$ -*N*-aminolactam structure.

Use of the nuclear Overhauser effect has also allowed us to determine for the first time the stereochemistry of the exocyclic C<sub>3</sub>=C<sub>8</sub> double bond in the condensed 5-membered *N*-aminolactams **3a–c**. Reliable information related to the spatial structure of these compounds was not available before.<sup>10,11</sup> In particular, the 2D NOESY spectrum clearly

(13) Yamaguchi, M.; Koga, T.; Kamei, K.; Akima, M.; Maruyama, N.; Kuroki, T.; Hamana, M.; Ohi, N. *Chem. Pharm. Bull.* **1994**, *42*, 1850.

(14) Yamaguchi, M.; Kamei, K.; Koga, T.; Akima, M.; Kuroki, T.; Ohi, N. *J. Med. Chem.* **1993**, *36*, 4052.

(15) (a) Dyck, B.; Markison, S.; Zhao, L.; Tamiya, J.; Grey, J.; Rowbottom, M. W.; Zhang, M.; Vickers, T.; Sorensen, K.; Norton, C.; Wen, J.; Heise, C. E.; Saunders, J.; Conlon, P.; Madan, A.; Schwarz, D.; Goodfellow, V. S. *J. Med. Chem.* **2006**, *49*, 3753. (b) Sotelo, E.; Coelho, A.; Ravina, E. *Tetrahedron Lett.* **2001**, *42*, 8633. Frank, H.; Heinisch, G.; Pharmacologically active pyridazines. In: Ellis, G.P.; West, G.B.; Editors, *Progress in Medicinal Chemistry*; Elsevier: Amsterdam, The Netherlands, 1990; p 1.

(16) Sonogashira, K.; Tohda, Y.; Hagihara, N. A. *Tetrahedron Lett.* **1975**, *50*, 4467.

(17) Brandsma, L.; Vasilevsky, S. F.; Verkruijse, H. D. *Application of Transition Metal Catalysts in Organic Synthesis*; Springer-Verlag: New York, 1998; p 335.

(18) Vasilevsky, S. F.; Shvartsberg, M. S. *Izv Akad. Nauk SSSR, Ser. Khim.* **1990**, *9*, 2089.

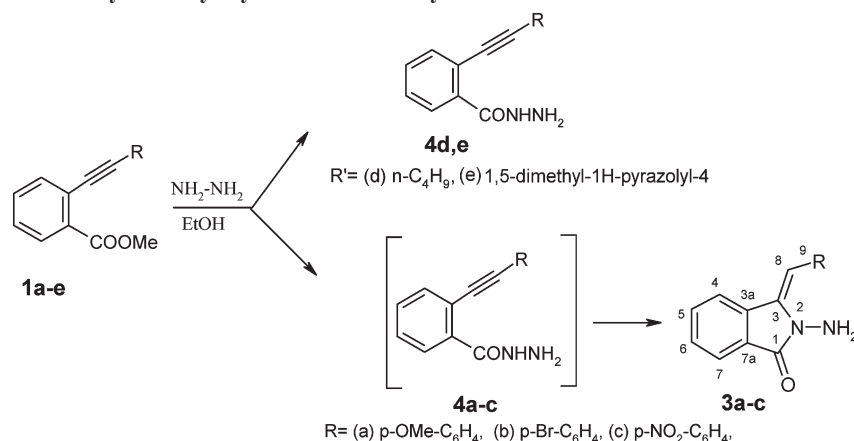
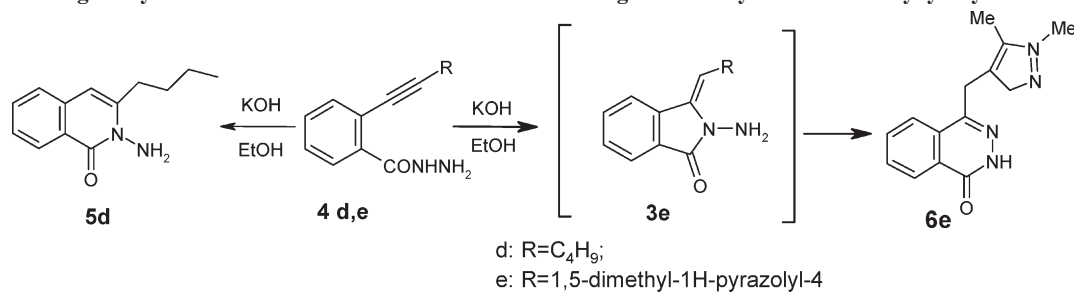
SCHEME 4. Interaction of Methyl *o*-Acetylenylbenzoates with HydrazineSCHEME 5. Divergent Synthesis of Two Classes of Six-Membered Nitrogen Heterocycles from *o*-Alkynyl Hydrazides **4d,e**

TABLE 1. Comparison of Experimental and Calculated (GIAO-B3LYP/6-311+G\*\* and GIAO-mPW1PW91/6-31G\*\* levels (in parentheses) on B3LYP/6-31+G\*\* geometry) Chemical Shifts of  $\text{H}^4$  and  $\text{H}^8$  for *E*- and *Z*-Forms of **3a**<sup>a</sup>

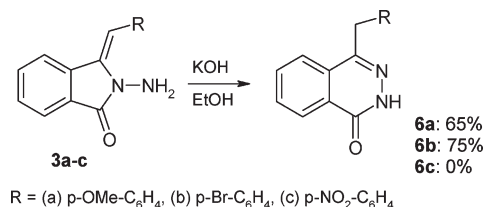
atom	experiment	calculation for <i>Z</i> -isomer	calculation for <i>E</i> -isomer
H-4	7.69	7.81 (7.77)	8.45 (8.28)
H-8	6.65	6.63 (6.36)	7.27 (7.26)

<sup>a</sup>See Scheme 4 for the atom numbering scheme.

displayed cross-peaks between  $\text{H}_4\text{--H}_8$  and  $\text{H}_{11,13}\text{--OCH}_3$  protons. The respective cross-peaks can only be explained by substantial Overhauser effect as the result of spatial proximity of these protons, which is only possible for  $\text{H}_4$  and  $\text{H}_8$  protons in the *Z*-configuration. This is an interesting observation because the observed *Z*-isomer is expected to be less stable than the nonobserved *E*-isomer (vide infra).

The spatial structure of lactam **3a** was additionally confirmed by the DFT calculation of proton NMR chemical shifts (Table 1). The mPW1PW91 functional with polarization basis set (e.g., 6-31G\*) was used extensively for reproducing experimental  $^1\text{H}$  and  $^{13}\text{C}$  NMR data<sup>19</sup> although NMR computations often required a higher basis set. Thus, NMR results were obtained from both mPW1PW91 and B3LYP computations as shown in Table 1. Not only are the

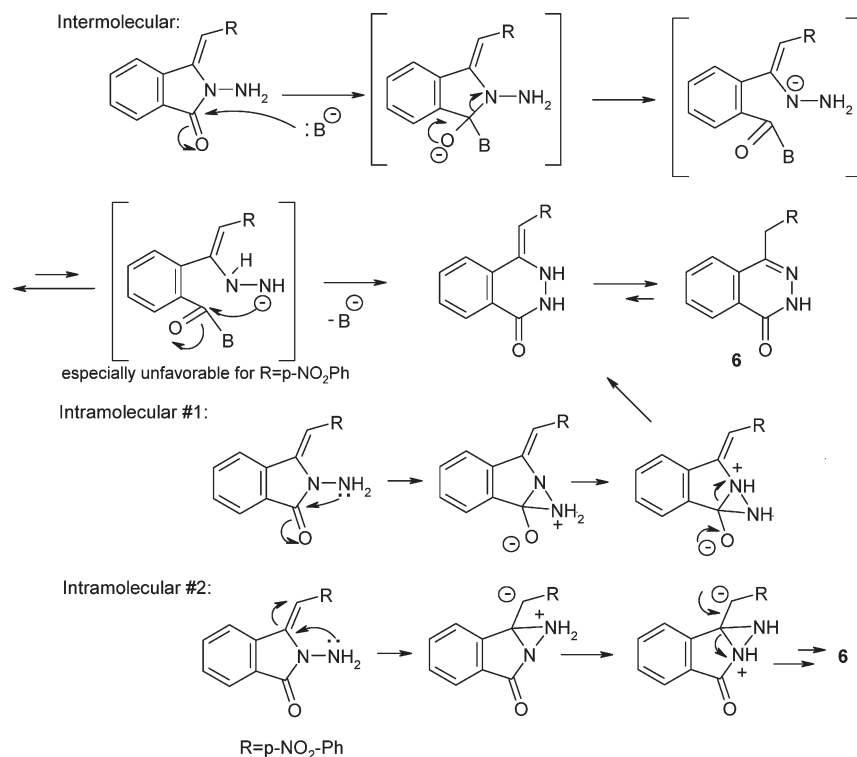
(19) Selected references discussing NMR computations at the MPW1PW91 level: Rychnovsky, S. D. *Org. Lett.* **2006**, *8*, 2895. Cimino, P.; Gomez-Paloma, L.; Duca, D.; Riccio, R.; Bifulco, G. *Magn. Reson. Chem.* **2004**, *42*, S26. Wojciech, M.; Barbara, R. *Magn. Reson. Chem.* **2004**, *42*, 459. Yang, J.; Huang, S.-X.; Zhao, Q.-S. *J. Phys. Chem. A* **2008**, *112*, 12132. For a general discussion, see also: Tuttle, T.; Kraka E.; Wu, A.; Cremer, D. *J. Am. Chem. Soc.* **2004**, *126*, 5093.

SCHEME 6. Base-Catalyzed Rearrangement of *N*-Amino Lactams into Benzopyridazinones

differences in the chemical shifts of these protons calculated for the *E*- and *Z*-configurations significant, but the experimental data agree much better with the calculated data for the *Z*-configuration. As a result, we conclude that quantum-mechanical calculations in these systems reliably confirm stereochemical assignments of **3a** and agree fully with the NOESY spectra.

Because reaction of the butyl derivative **1d** with hydrazine stopped at the stage of an open hydrazide **4d**, we repeated this experiment using a stronger base—KOH. The result was unexpected—for the first time for these benzoic acid derivatives, a six-membered *N*-amino lactam **5d** was formed via a 6-endo cyclization (75%). Note that this product is structurally different from the formal 6-exo-product **6** observed for the cyclization of a hetaryl-substituted acetylene **4e** (Scheme 5).

To test whether the formation of diazinone **6** proceeds through a rearrangement, we refluxed other *N*-amino lactams **3a-c** in ethanol in the presence of KOH (Scheme 6). Under these conditions, both lactams **3a,b** were converted into the analogous benzopyridazinones **6a,b** in 65% and

SCHEME 7. Suggested Mechanism for the Base-Catalyzed Rearrangement of *N*-Amino Lactams 3 into Benzopyridazinones 6

75% yields, respectively. Only lactam **3c** with a strong acceptor nitro substituent did not undergo recyclization even under more prolonged heating with KOH.

Proposed mechanisms for the rearrangement are outlined in Scheme 7. At the first step, the highly polarized carbonyl group is attacked by an external nucleophile. Subsequent collapse of the tetrahedral intermediate with concomitant cleavage of the C–N bond not only opens the cycle but also transforms the hydrazide moiety into conjugated base of a vinyl hydrazine. Unlike the hydrazide reactant, the hydrazine intermediate should have a relatively small difference in basicity between the internal and external nitrogen atoms.<sup>20</sup> Similar stability of the two conjugate nitrogen bases should enable their equilibration through proton transfer to the internal nitrogen atom. 6-Exo-trig attack of the terminal nitrogen anion at the carbonyl moiety furnishes the cyclic framework of the final product. Expulsion of the external nucleophile from the second tetrahedral intermediate followed by another prototropic isomerization affords the final product **6** (Scheme 7).

The equilibrium between the two conjugate bases of opened vinyl hydrazine is likely to be important for the success of recyclization. In particular, this equilibrium provides a simple explanation of why the *p*-nitro substitution stops the rearrangement. An acceptor substituent will shift the equilibrium away from the external anion and disfavor all reactions which originate from this intermediate.

(20) Note, however, that the equilibrium still should be shifted toward the vinyl hydrazide anion and, thus, be unfavorable for the recyclization. This notion may explain the absence of the rearrangement for X = *p*-NO<sub>2</sub>-Ph where the initially formed hydrazide anion will be additionally stabilized by the electron acceptor and, thus, the prototropic equilibrium will be even less favorable for the rearrangement.

We also considered the two intramolecular versions of this mechanism where exocyclic nitrogen serves as a nucleophile. These mechanisms, as shown in Scheme 7, are disfavored by high strain in the tricyclic aziridine intermediates, both of which do not correspond to a local energy minima at the B3LYP/6-31+G(d,p) potential energy surface (vide infra). Moreover, the intramolecular path 2 is further disfavored by the experimentally observed absence of rearrangement for R = *p*-NO<sub>2</sub>. On the basis of these considerations, the intermolecular version of the process presents itself as a more likely scenario. In any case, independent of the exact mechanism, such recyclization of  $\gamma$ -*N*-amino lactams into benzodiazinones under treatment with KOH is a previously unknown rearrangement.

We believe that such an isomerization can serve as a convenient synthetic approach toward pharmacologically important phthalazinones,<sup>21–23</sup> because the current literature methods require multistep procedures which involve either organometallic reagents, anhydrous media and high temperatures (up to 200 °C), or highly reactive chemicals such as SOCl<sub>2</sub>.<sup>13</sup>

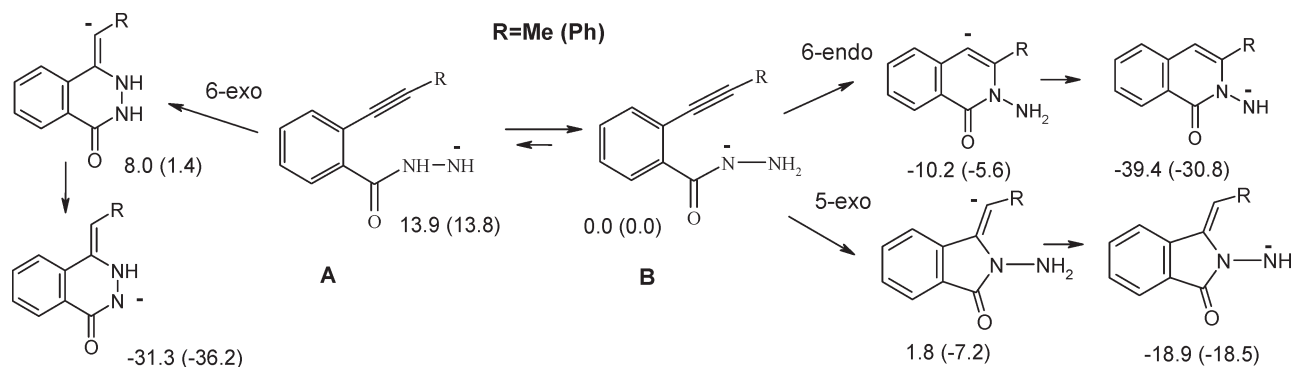
It is worth noting that cyclization of all positional isomers of hydrazides of *o*-acetylenyl pyrazolcarboxylic acids under basic conditions always led to 6-membered *N*-amino lactams.<sup>5,24</sup> These differences in the direction

(21) Loh, V. M. Jr.; Cockcroft, X. L.; Dillon, K. J.; Dixon, L.; Drzewiecki, J.; Eversley, P. J.; Gomez, S.; Hoare, J.; Kerrigan, F.; Matthews, I. T. W.; Menear, K. A.; Martin, N. M. B.; Newton, R. F.; Paul, J.; Smith, G. C. M.; Vile, J.; Whittle, A. J. *Bioorg. Med. Chem. Lett.* **2005**, *15*, 2235.

(22) Cockcroft, X. L.; Dillon, K. J.; Dixon, L.; Drzewiecki, J.; Kerrigan, F.; Loh, V. M. Jr.; Martin, N. M. B.; Menear, K. A.; Smith, G. C. M. *Bioorg. Med. Chem. Lett.* **2006**, *16*, 1040.

(23) del Olmo, E.; Barroza, B.; Ybarra, M. I.; Lopez-Perez, J. L.; Carron, R.; Sevilla, M. A.; Boselli, C.; San Feliciano, A. *Bioorg. Med. Chem. Lett.* **2006**, *16*, 2786.

(24) Vasilevsky, S. F.; Mshvidobadze, E. V.; Elguero, J. *Heterocycles* **2002**, *57*, 2255.

**SCHEME 8. Substituent Effects on the Relative Stabilities of Key Anionic Intermediates for R = Me and Ph at the B3LYP/6-31+G(d,p) Level<sup>a</sup>**


<sup>a</sup>All values for the gas phase relative to the hydrazide anion, data for R = Ph are given in parentheses.

and feasibility of cycloisomerization stimulated us to investigate this reaction and related processes through a detailed quantum mechanical study. Computational analysis was used to understand the nature of factors controlling the relative rates of 5-exo, 6-endo, and 6-exo cyclization paths, to ascertain the feasibility of direct 6-exo closure and relative stability of the anionic precursor for this process, and to dissect stereoelectronic effects controlling the relative stability of cyclic anionic intermediates and reaction stereoselectivity. These results will be used to validate our interpretation of experimental findings and to benchmark the accuracy of computational models for these types of anionic cyclizations.

**Description of Computational Approach.** Calculations were performed by using Gaussian 03 software<sup>25</sup> with geometries and energies obtained at the B3LYP/6-31+G(d,p) level of theory.<sup>26</sup> All stationary point geometries for the anionic cyclizations were optimized at the B3LYP/6-31+G\*\* level. Reactants, products, and intermediates were confirmed as minima and the transition state structures were confirmed as saddle points with a single imaginary frequency through frequency calculations. The solvation effects were tested by single point energy calculations with PCM model at the SCRFB3LYP/6-31+G\*\* level in ethanol at the respective gas phase geometries. Energies of hyperconjugative interactions were calculated by using the Natural Bond Orbital (NBO)<sup>27</sup> method implemented in Gaussian. The Nucleus Independent Chemical Shift (NICS) values were evaluated at 1 Å above the center of the ring planes by using the GIAO<sup>28</sup> approach.

All energies at  $T = 0$  were calculated with the zero-point vibration (ZPVE) and thermal correction (TCE) energies.<sup>29</sup> Solvation effects were calculated at the PCM-SCRFB3LYP/6-31+G(d,p)//B3LYP/6-31+G(d,p) level, using geometries and frequencies obtained from the gas phase calculations.

Because the calculated activation barrier for the 5-exo cyclization reaction of the neutral hydrazides was found to be prohibitively large ( $\sim 50$  kcal/mol), all calculations were performed for the anionic form of the reagent. The relative acidity of hydrazides suggests that this form is sufficiently populated under the reaction conditions.<sup>30</sup>

Intrinsic and thermodynamic contributions to the reaction barrier were separated by using Marcus theory.<sup>31</sup> This analysis allows one to compare inherent stereoelectronic requirements of reactions with different thermodynamic driving forces by comparing their intrinsic barriers separated from the thermodynamic contribution. Intrinsic activation energy,  $E_o$ , is determined from the following equation:  $E_o = [E_a - 1/2\Delta E_R + (E_a^2 - E_a\Delta E_R)^{1/2}]/2$ , where  $E_a$  = activation energy and  $\Delta E_R$  = reaction energy.

**Computational Results.** To rationalize the observed experimental results and gain a deeper insight into the nature of electronic effects responsible for the formation of three different families of heterocycles from the same common class of precursors, we concentrated on several questions: (a) relative stabilities of anions at the two adjacent nitrogen atoms in hydrazides and vinyl hydrazines (thermodynamic control), (b) relative barriers for the alternative cyclization paths (kinetic control), and (c) relative stability of cyclic intermediates and final products and its correlation with hyperconjugative stereoelectronic effects (stereochemical preferences).

**Relative Stability of Acyclic Anions and Cyclic Anions.** As expected, the adjacent carbonyl group provides strong

(30) Zhao, Y.; Bordwell, F. G.; Cheng, J. P.; Wang, D. *J. Am. Chem. Soc.* **1997**, *119*, 9125. Due to the presence of hydrazine in the reaction medium ( $K_B = [N_2H_5^+][OH^-]/[N_2H_4] = 10^{-5.9}$  at room temperature), the reaction medium has substantial basic character (pH  $\sim 11$  at  $[N_2H_4] \approx 1$  M). National Institute of Standards and Technology (NIST). Computational Chemistry Comparison and Benchmark Data Base (CCCBDB): <http://srdata.nist.gov/cccbdb/>.

(31) Marcus, R. A. *Annu. Rev. Phys. Chem.* **1964**, *15*, 155. Marcus, R. A. *J. Phys. Chem.* **1968**, *72*, 891. Selected applications to different classes of chemical reactions: Chen, M. Y.; Murdoch, J. R. *J. Am. Chem. Soc.* **1984**, *106*, 4735. Wolfe, S.; Mitchell, J.; Schlegel, H. B. *J. Am. Chem. Soc.* **1981**, *103*, 7694. Newcomb, M.; Johnson, C. C.; Makek, M. B.; Varick, T. R. *J. Am. Chem. Soc.* **1992**, *114*, 10915. Martinesker, A. A.; Johnson, C. C.; Horner, J. H.; Newcomb, M. *J. Am. Chem. Soc.* **1994**, *116*, 9174. Guthrie, J. P.; Guo, J. N. *J. Am. Chem. Soc.* **1996**, *118*, 11472. Guthrie, J. P. *J. Am. Chem. Soc.* **2000**, *122*, 5529. Lewis, F. D.; Kalgutkar, R. S.; Wu, Y.; Liu, X.; Liu, J.; Hayes, R. T.; Miller, S. E.; Wasielewski, M. R. *J. Am. Chem. Soc.* **2000**, *122*, 12346. Newcomb, M.; Makek, M. B.; Glenn, A. G. *J. Am. Chem. Soc.* **1991**, *113*, 949. Yoo, H. Y.; Houk, K. N. *J. Am. Chem. Soc.* **1997**, *119*, 2877. Alabugin, I. V.; Manoharan, M.; Breiner, B.; Lewis, F. *J. Am. Chem. Soc.* **2003**, *125*, 9329.

(25) Frish, M. J. et al., *Gaussian 03*, Revision E.01; Gaussian, Inc., Wallingford CT, 2004.

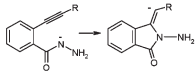
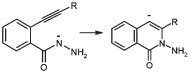
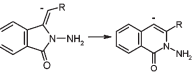
(26) Becke, A. D. *J. Chem. Phys.* **1993**, *98*, 5648.

(27) The NBO 4.0 Program: Glendening, E. D.; Badenhoop, J. K.; Reed, A. E.; Carpenter, J. E.; Weinhold, F. Theoretical Chemistry Institute, University of Wisconsin, Madison, WI, 1996.

(28) Wolinski, K.; Hilton, J. F.; Pulay, P. *J. Am. Chem. Soc.* **1990**, *112*, 8251.

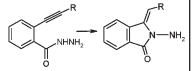
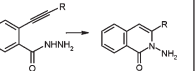
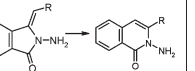
(29) Hehre, W. J.; Ditchfield, R.; Radom, L.; Pople, J. A. *J. Am. Chem. Soc.* **1970**, *92*, 4796.

TABLE 2. Reaction Energies for the Anionic 5-Exo and 6-Endo Closures and Formal 5-Exo → 6-Endo Isomerization at the PCM-SCRF B3LYP/6-31+G(d,p)//B3LYP/6-31+G(d,p) Level of Theory<sup>a</sup>

R				
$\Delta E_T^{gas}$	C <sub>4</sub> H <sub>9</sub>	-0.42	-9.19	-8.77
	C <sub>6</sub> H <sub>4</sub> OCH <sub>3</sub>	-4.44	-4.72	-0.29
	C <sub>6</sub> H <sub>5</sub>	-6.78	-5.12	1.66
	C <sub>6</sub> H <sub>4</sub> Br	-9.12	-6.79	2.33
	C <sub>6</sub> H <sub>4</sub> NO <sub>2</sub>	-17.90	-8.20	9.70
$\Delta E_T^{solv}$	C <sub>4</sub> H <sub>9</sub>	4.86	-6.34	-11.19
	C <sub>6</sub> H <sub>4</sub> OCH <sub>3</sub>	1.15	-1.88	-3.02
	C <sub>6</sub> H <sub>5</sub>	-1.29	-2.03	-0.74
	C <sub>6</sub> H <sub>4</sub> Br	-3.08	-3.21	-0.13
	C <sub>6</sub> H <sub>4</sub> NO <sub>2</sub>	-14.28	-4.24	10.04

<sup>a</sup>The data are given for  $T = 298.15$  K, solvent = ethanol; all energies are in kcal/mol.

TABLE 3. Reaction Energies for the Formal 5-Exo and 6-Endo Closures and 5-Exo → 6-Endo Isomerization of the Neutral Hydrazides at the PCM-SCRF B3LYP/6-31+G(d,p)//B3LYP/6-31+G(d,p) Level of Theory<sup>a</sup>

R				
$\Delta E_T^{gas}$	C <sub>4</sub> H <sub>9</sub>	-29.83	-42.03	-12.20
	C <sub>6</sub> H <sub>4</sub> OCH <sub>3</sub>	-26.96	-37.45	-10.48
	C <sub>6</sub> H <sub>5</sub>	-27.24	-37.74	-10.50
	C <sub>6</sub> H <sub>4</sub> Br	-28.17	-38.33	-10.16
	C <sub>6</sub> H <sub>4</sub> NO <sub>2</sub>	-28.93	-38.14	-9.21
$\Delta E_T^{solv}$	C <sub>4</sub> H <sub>9</sub>	-29.73	-41.59	-11.85
	C <sub>6</sub> H <sub>4</sub> OCH <sub>3</sub>	-27.19	-37.07	-9.88
	C <sub>6</sub> H <sub>5</sub>	-27.33	-37.39	-10.06
	C <sub>6</sub> H <sub>4</sub> Br	-29.57	-38.15	-9.71
	C <sub>6</sub> H <sub>4</sub> NO <sub>2</sub>	-25.40	-38.03	-12.63

<sup>a</sup>The data are given for  $T = 298.15$  K, solvent = ethanol; all energies are in kcal/mol.

stabilization to the anionic center, imparting larger stability to the  $\alpha$ -anion. The calculated ca. 14 kcal/mol difference in stability does not depend strongly on the nature of substituent at the triple bond. As a result, all cyclizations of the less stable  $\beta$ -anion have to carry an additional energy penalty and, thus, are unlikely to be competitive unless their activation energies are sufficiently low to overcome this handicap (vide infra) (Scheme 8).

Interestingly, the cyclic carbanions have relatively high energy and several of the calculated ring closures are predicted to be endothermic. This finding contrasts sharply with the high exothermicity of analogous cyclizations of carbon centered reactive species<sup>32</sup> where the gain in stability due to the transformation of a relatively weak acetylenic  $\pi$ -bond into a stronger  $\sigma$ -bond is not partially offset by the concomitant transformation of a relatively stable nitrogen anion

into a less stable carbanion. On the other hand, exothermicity of the anionic cyclizations is increased dramatically upon prototropic isomerization of the initially formed carbanions into  $N$ -anions. The computational data suggest that such tautomerizations are likely to play the key role in driving these cyclizations to completion.

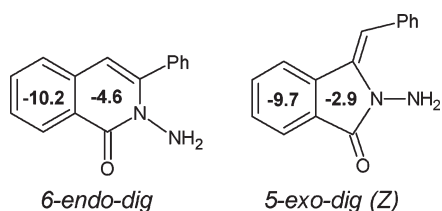
Overall, the calculated energies suggest that the formal 6-exo product for  $R = Ph$  and 6-endo product for  $R = alkyl$  are likely to be formed under thermodynamic control conditions leading to the formation of the most stable product. Substituent effects at the relative enthalpies for the formation of 5-exo and 6-endo products in their anionic form at  $T = 298.15$  K are given in Table 2. The calculated energetic preference for the formation of six-membered cycles suggests that the experimental preference for the formation of the 5-membered cycle for  $R = C_6H_4OCH_3, C_6H_5, C_6H_4Br, C_6H_4NO_2$  results from kinetic, rather from thermodynamic, control. In accord with the experimental results, computations suggest that formation of the five-membered products is most favorable for the aromatic substituents whereas

(32) See for example: Alabugin, I. V.; Manoharan, M. *J. Am. Chem. Soc.* **2005**, *127*, 95345. Kovalenko, S. V.; Peabody, S.; Manoharan, M.; Clark, R. J.; Alabugin, I. V. *Org. Lett.* **2004**, *6*, 2457. Also see refs 4 and 9.

**TABLE 4.** Computed Activation and Reaction Energies for Competing Anionic Cyclizations of the Two Conjugate Bases of Aryl Hydrazides at the B3LYP/6-31+G\*\* Level<sup>a</sup>

Compound R = Me (Ph)	RE, kcal/mol	Mode	E <sub>a</sub> (gas) kcal/mol	E <sub>a</sub> (solv), kcal/mol	ΔE <sub>r</sub> (gas), kcal/mol	ΔE <sub>r</sub> (solv), kcal/mol	E <sub>0</sub> (gas) kcal/mol
	0.0 (0.0) 0.0 (0.0) <sup>e</sup>	6-endo-dig (B→B1)	12.0 (14.9)	16.1 (19.4)	-10.2 (-5.6)	-8.2 (-2.5)	16.7 (17.6)
		5-exo-dig (Z) <sup>b,d</sup> (B→B2)	11.4 (7.8)	16.2 (12.5)	1.8 (-7.2)	5.7 (-1.6)	10.5 (11.1)
		5-exo-dig (E) <sup>b,d</sup> (B→B1)	18.4 (8.6)	22.0 (13.0)	-2.6 (-10.2)	2.1 (-4.1)	19.7 (13.2)
	13.9 (13.8) 13.2 (14.4) <sup>e</sup>	6-exo-dig (Z) <sup>a,c</sup> (A→A2)	16.7 (15.3)	19.0 (17.9)	-5.9 (-12.4)	-2.5 (-9.3)	19.5 (21.0)
		6-exo-dig (E) <sup>a,c</sup> (A→A1)	16.9 (16.2)	20.3 (15.3)	0.2 (-10.2)	-0.8 (-8.5)	16.8 (21.0)

<sup>a</sup>Z-isomer is more stable than E-isomer by 6.1 (2.3) kcal/mol. <sup>b</sup>Z-isomer is more stable than E-isomer by 4.5 (3.0) kcal/mol. <sup>c</sup>The Z-isomer of protonated product is less stable than E-isomer by 0.2 (1.9) kcal/mol. <sup>d</sup>The Z-isomer of protonated product (experimentally observed) is less stable than E-isomer than E by 1.9 (2.7) kcal/mol. <sup>e</sup>Computed from PCM-SCRF solvation model. <sup>a</sup>R = methyl and phenyl (values in parentheses). Solvation effects are estimated with single point PCM-SCRF B3LYP/6-31+G\*\*//B3LYP/6-31+G\*\* calculations. E<sub>0</sub> corresponds to the intrinsic activation energy obtained from the Marcus equation. See Figure 2 for the product structures.

**FIGURE 1.** Nucleus independent chemical shift (NICS(1) in ppm) data for the products of 5-exo-dig and 6-endo-dig cyclizations computed at the B3LYP/6-311+G\*\*//B3LYP/6-31+G\*\* level.

formation of the six-membered product may be expected for R = alkyl. As expected, the relative stability of the five-membered cycle increases in parallel to the increase of acceptor ability of substituent R (R = C<sub>4</sub>H<sub>9</sub> → C<sub>6</sub>H<sub>4</sub>OCH<sub>3</sub> → C<sub>6</sub>H<sub>5</sub> → C<sub>6</sub>H<sub>4</sub>Br → C<sub>6</sub>H<sub>4</sub>NO<sub>2</sub>).

Again, all anionic cyclizations in Table 2 do not have the strong thermodynamic driving force due to the unfavorable transformation of a nitrogen anion into a less stable carbanion. Interestingly, inclusion of solvation further decreases exothermicities of these cyclizations and even renders some of them endothermic. The lower yield of the 5-exo cyclization for R = *p*-OMe-Ph (67%) is consistent with the prediction that this reaction is essentially thermoneutral, whereas the higher yielding 5-exo cyclizations for R = *p*-Br-Ph, *p*-NO<sub>2</sub>-Ph (~90%) are predicted to be noticeably exothermic.

For the neutral acyclic starting materials and cyclized products, the relative energies (Table 3) do not bear the above energy penalty for the transformation of nitrogen anions into carbanions. As a result, the relative trends in stability for the neutral molecules more accurately reflect the gain in stability due to the conversion of acetylenic π-bonds into stronger C–N σ-bonds. Consequently, the stability of the cyclic products relative to the acyclic starting materials increases significantly in comparison to their anionic counterparts in Table 2. Although formation of both five- and six-membered cycles is exothermic, the 6-membered cycles are more stable. The relative stability of cyclic compounds correlates with the donor–acceptor properties of substituent

R. In particular, as the acceptor properties increase in the series R = C<sub>4</sub>H<sub>9</sub> → C<sub>6</sub>H<sub>4</sub>OCH<sub>3</sub> → C<sub>6</sub>H<sub>5</sub> → C<sub>6</sub>H<sub>4</sub>Br → C<sub>6</sub>H<sub>4</sub>NO<sub>2</sub>, the relative stability of the six-membered cycle decreases. The analogous dependence, with the exception of R = C<sub>4</sub>H<sub>9</sub>, is observed for the cycle formation: exothermicity for the five- and six-membered-ring formation increases in the R = C<sub>6</sub>H<sub>4</sub>OCH<sub>3</sub> → C<sub>6</sub>H<sub>5</sub> → C<sub>6</sub>H<sub>4</sub>Br → C<sub>6</sub>H<sub>4</sub>NO<sub>2</sub> series.

Higher stability of the 6-endo products can be explained by greater aromaticity of the newly formed ring, as suggested by the more negative Nucleus Independent Chemical Shift (NICS) values in Figure 1. The NICS value at a distance of 1 Å from the ring centers (NICS(1) value) is a convenient magnetic measure of aromaticity that generally correlates with aromatic stabilization as well.<sup>33</sup> Typically, more negative NICS found at the center of ring systems indicates the presence of diatropic ring current and an aromatic system whereas positive NICS indicates paramagnetic ring current and antiaromaticity.

**Kinetic Competition between 5-Exo-, 6-Endo-, and 6-Exo Cyclizations.** Potential energy surfaces for the three anionic closures (5-exo, 6-endo, and 6-exo) for the parent aryl-substituted hydrazide (R = Ph) are presented in Figure 2. The 5-exo-dig closure is clearly kinetically favored in this system. Interestingly, although the activation barrier is lower for the formation of the Z-isomer of the cyclic anion **B2** (corresponding to the experimentally observed Z-product), the E-form of the cyclic anion **B3** is slightly more stable in the product (we will discuss the origin of this effect in the following section). Because the 5-exo cyclization is 7–10 kcal/mol exothermic, ring-opening of the 5-exo product should be relatively slow, thus providing additional time for the prototropic isomerization into a nitrogen-centered anion **B4** to occur. The 6-endo-dig cyclization has a noticeably higher barrier (~15 kcal/mol) and should be kinetically

(33) For the details of NICS calculations, see: Schleyer, P. v. R.; Maerker, C.; Dransfeld, A.; Jiao, H.; van Eikema Hommes, N. J. R. *J. Am. Chem. Soc.* **1996**, *118*, 6317. Schleyer, P. v. R.; Manoharan, M.; Wang, Z. X.; Kiran, B.; Jiao, H.; Puchta, R.; van Eikema Hommes, N. J. R. *Org. Lett.* **2001**, *3*, 2465.



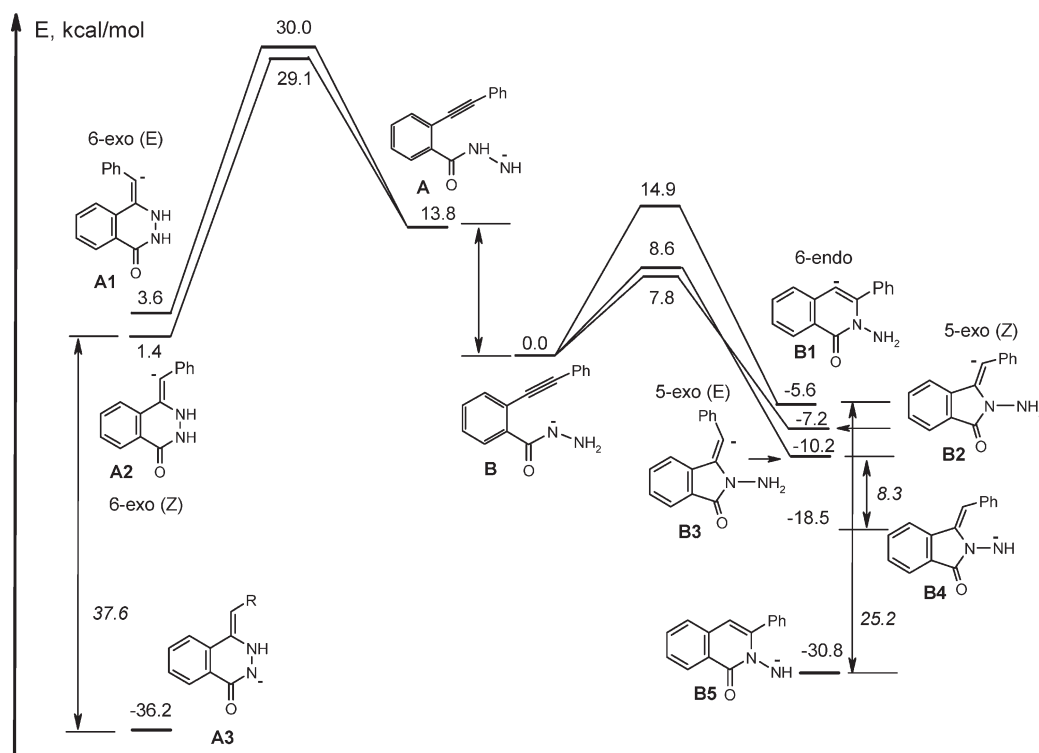


**FIGURE 2.** Full potential energy surface for the competing 6-endo, 5-exo, and 6-exo anionic cyclizations of hydrazide anions **A** and **B**. All energies of stationary point geometries are given relative to the most stable hydrazide anion (compound **B** in Scheme 8) at the B3LYP/6-31+G\*\* level.

disfavored compared to the 5-exo-dig cyclizations ( $E_a = 8-9$  kcal/mol).

The  $\sim 15$  kcal/mol barrier for 6-exo-dig cyclization of the  $\beta$ -anion is comparable to the barrier for the 6-endo-dig closure of the  $\alpha$ -anion **B**. However, the lower stability of the  $\beta$ -anion **A** raises the overall 6-exo cyclization barrier up to ca. 29 kcal/mol (according to the Curtin–Hammett principle). Since both 5-exo and 6-endo barriers for the  $\alpha$ -anion cyclizations are much lower, the formal 6-exo products **A1** and **A2** described in Scheme 6 cannot be accessed directly from the acyclic hydrazide anion under the kinetic control conditions. Instead, the formal 6-exo products stem from an alternative rearrangement path discussed earlier (Scheme 7). Tautomerization of the 6-exo products into a nitrogen-centered anion **A3** provides the most stable structure on the overall potential energy surface ( $\sim 36$  kcal/mol lower than the hydrazide  $\alpha$ -anion **B** and  $\sim 50$  kcal/mol lower than the  $\beta$ -anion **A**).

Activation energies summarized in Table 4 clearly show that substituents at the alkyne moiety have a strong effect on the competition between the 5-exo and 6-endo cyclization of the  $\alpha$ -anion. Decreased 5-exo-dig activation energies and increased stability of the 5-exo products for  $R = \text{Ph}$  confirm that the Ph group steers the cyclization selectively down the 5-exo path by providing benzylic stabilization to the anionic center in the product. In contrast, the competition between the 5-exo and 6-endo-dig closures is rather close for  $R = \text{Me}$ . In this case, the values of cyclization barriers are within 1 kcal/mol of each other and thus both cyclizations can proceed with comparable rates. Although the 5-exo cyclization has a 0.6 kcal/mol lower barrier than the 6-endo closure in the gas phase, introduction of solvation reverses this subtle

preference. Moreover, the 5-exo-dig cyclization is predicted to be endothermic and readily reversible in this case, whereas the 6-endo-dig closure is  $\sim 10$  kcal/mol exothermic.

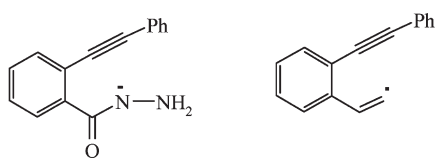
Higher values for the computed activation barriers for both cyclizations of alkyl-substituted alkynes are consistent with our ability to isolate the hydrazide intermediate under the conditions where aryl-substituted substrates undergo fast 5-exo closure (Scheme 4). Overall, computational results are in excellent agreement with the experimental observations.

The above reactions of anionic nucleophiles are less exothermic than the topologically similar cyclizations of other reactive intermediates.<sup>34</sup> To understand the role of thermodynamic factors on the cyclization rates and to compare intrinsic stereoelectronic factors involved in the three cyclizations, we separated intrinsic barriers ( $E_0$  in Table 4) from the variable thermodynamic contributions using Marcus theory. We have used this approach in the past for the analysis of radical cyclizations of alkynes.<sup>34</sup> The present work provides the first application of this approach to anionic cyclizations.

A more detailed comparison of calculated activation barriers and their intrinsic components of 5-exo and 6-endo anionic cyclization with the same parameters for the topologically analogous cyclizations of vinyl radicals is given in Scheme 9. Both anionic cyclizations are predicted to be much slower than the radical processes despite the obvious similarity in the cyclization patterns. Marcus dissection clearly illustrates that the reason for the higher barriers for the

(34) (a) Alabugin, I. V.; Manoharan, M. *J. Comput. Chem.* **2007**, *28*, 373. (b) Alabugin, I. V.; Manoharan, M. *J. Org. Chem.* **2004**, *69*, 9011. (c) Alabugin, I. V.; Manoharan, M.; Zeidan, T. A. *J. Am. Chem. Soc.* **2003**, *125*, 14014. (d) Alabugin, I. V.; Zeidan, T. A. *J. Am. Chem. Soc.* **2002**, *124*, 3175. (e) Alabugin, I. V. *J. Org. Chem.* **2000**, *65*, 3910.

**SCHEME 9. Comparison of Total and Intrinsic Activation Barriers (kcal/mol) for 5-Exo-Dig and 6-Endo-Dig Cyclizations of N-Anions and C-Radicals**



	5-exo:	6-endo:
$E_a$	7.8	14.9
$E_o$	11.1	17.6
	0.6	4.6
	13.8	24.8

anionic cyclizations lies in their lower exothermicity. Once the thermodynamic factors are removed, intrinsic barriers for these two anionic cyclizations become slightly lower than those for the radical counterparts. It is also interesting that, independent of the type of reaction species (nitrogen anion or carbon radical), the 5-exo-dig cyclization remains stereoelectronically preferred to the 6-endo-dig ring closure as evidenced by the lower intrinsic 5-exo barriers.

**The Origin of Z-Stereoselectivity in the 5-Exo Cyclizations and Competition of Stereoelectronic Hyperconjugative Effects in Cyclized Carbanions.** Our computational analysis yielded several interesting observations regarding relative energies of stereoisomeric anions formally corresponding to products of 5-exo and 6-exo-dig cyclizations. Although stereochemical information is lost during the prototropic isomerization of the formal 6-exo products into experimentally observed benzopyridazinones **6**, the 5-exo cyclization proceeds stereoselectively and affords only *Z*-isomer of the product. This result is fully consistent with the lower calculated barrier for the formation of the *Z*-isomer.

An unusual observation is that although the transition state energy for the 5-exo-dig cyclization leading to the *Z*-isomer is lower than that for the analogous cyclization of the *E*-isomer, the relative stability of the two cyclized anions is opposite to that of the transition states. Taking into account our long-standing interest in hyperconjugative stereoelectronic effects,<sup>34</sup> we analyzed delocalizing hyperconjugative interactions in the key anionic species using Natural Bond Orbital (NBO) analysis. Similar interactions which

**TABLE 5. Relative Energies of the Stereoisomers of the 5-Exo and 6-Exo Anionic Cyclization Products B2/B3 and A1/A2 along with Energies of Selected Hyperconjugative Interactions (B3LYP/6-31+G\*\*) <sup>a</sup>**

	5-exo ( <i>Z</i> )	5-exo ( <i>E</i> )	6-exo ( <i>Z</i> )	6-exo ( <i>E</i> )
relative energy	4.5 (3.0)	0.0 (0.0)	10.6 (11.6)	16.7 (13.9)
$E(n_C \rightarrow \sigma^*_{C-N})$	27.2 (24.8)	6.3 (7.9)	21.7 (21.5)	4.9 (7.8)
$E(n_C \rightarrow \sigma^*_{C-C})$	1.5 (2.8)	18.2 (17.1)	1.2 (2.4)	18.3 (17.4)
$E(n_C \rightarrow \sigma^*_{N-H})$	NA	11.2 (7.5)	NA	NA

<sup>a</sup>Energies are given in kcal/mol, data for R = Ph are in parentheses, structures are given in Scheme 10.

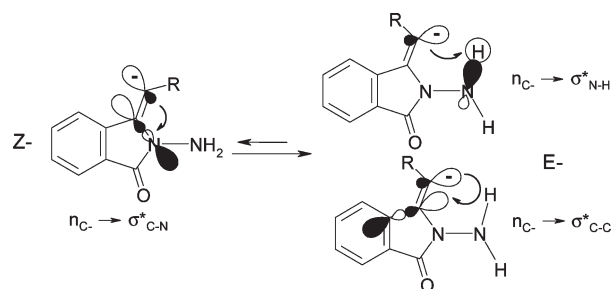


**FIGURE 3.** Competition of  $n_C \rightarrow \sigma^*_{C-N}$  vicinal hyperconjugation in the *Z*-anionic product of the 5-exo-dig closure and  $C \cdots H-N$  H-bonding and  $n_C \rightarrow \sigma^*_{C-C}$  vicinal hyperconjugation in the *E*-anion.

involve  $\sigma$  bonds manifest themselves in numerous stereoelectronic effects controlling organic structure and reactivity.<sup>35,36</sup> In particular, hyperconjugation influences conformational equilibria,<sup>37,38</sup> modifies reactivity,<sup>39</sup> determines selectivity,<sup>40</sup> and is enhanced dramatically in excited, radical, and ionic species.<sup>41</sup> In the following part, we will show that observed stereoselectivity stems from an interesting interplay of hyperconjugative effects which are developed to a different extent at the different stages of the cyclization process.

NBO analysis identified an extremely strong hyperconjugative  $n_C \rightarrow \sigma^*_{C-N}$  interaction of anionic carbon orbital and antiperiplanar acceptor C–N bond<sup>34d</sup> in the *Z*-isomer. The analogous interaction between these orbitals is significantly lower in the *E*-isomer due to the less favorable syn-arrangement of the two interacting orbitals. Evidently, this interaction is developed already in the TS providing a favorable stabilizing

(35) (a) Kirby, A. J. *The Anomeric Effect and Related Stereoelectronic Effects at Oxygen*; Springer-Verlag: Berlin, Germany, 1983. (b) *The Anomeric Effect and Associated Stereoelectronic Effects*; Thatcher, G. R. J., Ed.; ACS Symp. Ser. No. 539; American Chemical Society: Washington, DC, 1993. (c) Juaristi, E.; Guevas, G. *The Anomeric Effect*; CRC Press: Boca Raton, FL, 1994. (d) Reed, A. E.; Curtiss, L. A.; Weinhold, F. *Chem. Rev.* **1988**, *88*, 899. (e) Juaristi, E.; Cuevas, G. *Acc. Chem. Res.* **2007**, *40*, 961.

(36) Cohen, T.; Lin, M.-T. *J. Am. Chem. Soc.* **1984**, *106*, 1130. Danishefsky, S. J.; Langer, M. *Org. Chem.* **1985**, *50*, 3672. Rychnovsky, S. D.; Mickus, D. E. *Tetrahedron Lett.* **1989**, *30*, 3011. Vedejs, E.; Dent, W. H. *J. Am. Chem. Soc.* **1989**, *111*, 6861. Juaristi, E.; Cuevas, G.; Vela, A. *J. Am. Chem. Soc.* **1994**, *116*, 5796. Salzner, U.; Schleyer, P. v. R. *J. Org. Chem.* **1994**, *59*, 2138. Vedejs, E.; Dent, W. H.; Kendall, J. T.; Oliver, P. A. *J. Am. Chem. Soc.* **1996**, *118*, 3556. Cuevas, G.; Juaristi, E.; Vela, A. *THEOCHEM* **1997**, *418*, 231. Anderson, J. E.; Cai, J.; Davies, A. G. *J. Chem. Soc., Perkin Trans. 2* **1997**, 2633. Wiberg, K. B.; Hammer, J. D.; Castejon, H.; Bailey, W. F.; DeLeon, E. L.; Jarret, R. M. *J. Org. Chem.* **1999**, *64*, 2085. Juaristi, E.; Rosquete-Pina, G. A.; Vazquez-Hernandez, M.; Mota, A. *J. Pure Appl. Chem.* **2003**, *75*, 589.

(37) Juaristi, E., Ed. *Conformational Behavior of Six-Membered Rings*; VCH Publishers: New York, 1995. See also: Romers, C.; Altona, C.; Buys, H. R.; Havinga, E. *Top. Stereochem.* **1969**, *4*, 39. Zefirov, N. S.; Schechtman, N. M. *Usp. Khim.* **1971**, *40*, 593. Juaristi, E.; Cuevas, G. *Tetrahedron* **1992**, *48*, 5019. Graczyk, P. P.; Mikolajczyk, M. *Top. Stereochem.* **1994**, *21*, 159.

(38) (a) Reed, A. E.; Weinhold, F. *Isr. J. Chem.* **1991**, *31*, 277. (b) Goodman, L.; Pophristic, V.; Gu, H. *J. Chem. Phys.* **1999**, *110*, 4268. (c) Goodman, L.; Pophristic, V.; Weinhold, F. *Acc. Chem. Res.* **1999**, *32*, 983. (d) Schreiner, P. R. *Angew. Chem., Int. Ed.* **2002**, *41*, 3579. (e) Cramer, C. J. *THEOCHEM* **1996**, *370*, 135.

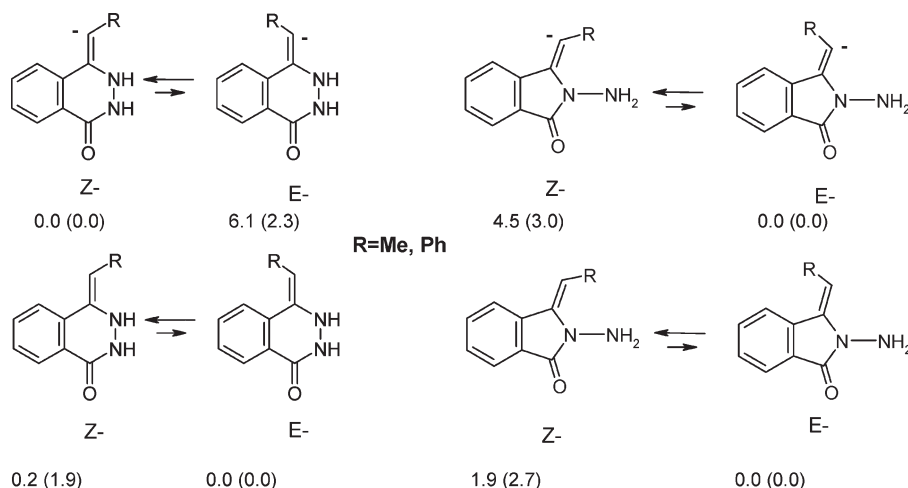
(39) Baddeley, G. *Tetrahedron Lett.* **1973**, *14*, 1645. Chang, J.-W. A.; Taira, K.; Urano, S.; Gorenstein, D. G. *Tetrahedron* **1987**, *43*, 479. Um, I. H.; Chung, E. K.; Lee, S. M. *Can. J. Chem.* **1998**, *76*, 729. Deslongchamps, P. *Tetrahedron* **1975**, *31*, 2463. Doddi, G.; Ercolani, G.; Mencarelli, P. *J. Org. Chem.* **1992**, *57*, 4431. Roberts, B. P.; Steel, A. J. *Tetrahedron Lett.* **1993**, *34*, 5167. Sato, M.; Sunami, S.; Kaneko, C. *Heterocycles* **1995**, *42*, 861 and references cited therein. Wagner, P. J.; Scheve, B. J. *J. Am. Chem. Soc.* **1977**, *99*, 1858. Lambert, J. B.; Zhao, Y.; Emblidge, R. W.; Salvador, L. A.; Liu, X.; So, J. -H.; Chelius, E. C. *Acc. Chem. Res.* **1999**, *32*, 18. Borden, W. T. *J. Chem. Soc., Chem. Commun.* **1998**, 1919. Maier, M. E. *Angew. Chem., Int. Ed.* **2000**, *39*, 2073. Klempeter, E.; Rolla, N.; Koch, A.; Taddei, F. *J. Org. Chem.* **2006**, *71*, 4393.

(40) Beckwith, A. L. J.; Duggan, P. J. *Tetrahedron*, **1998**, *54*, 6919 and the examples cited therein.

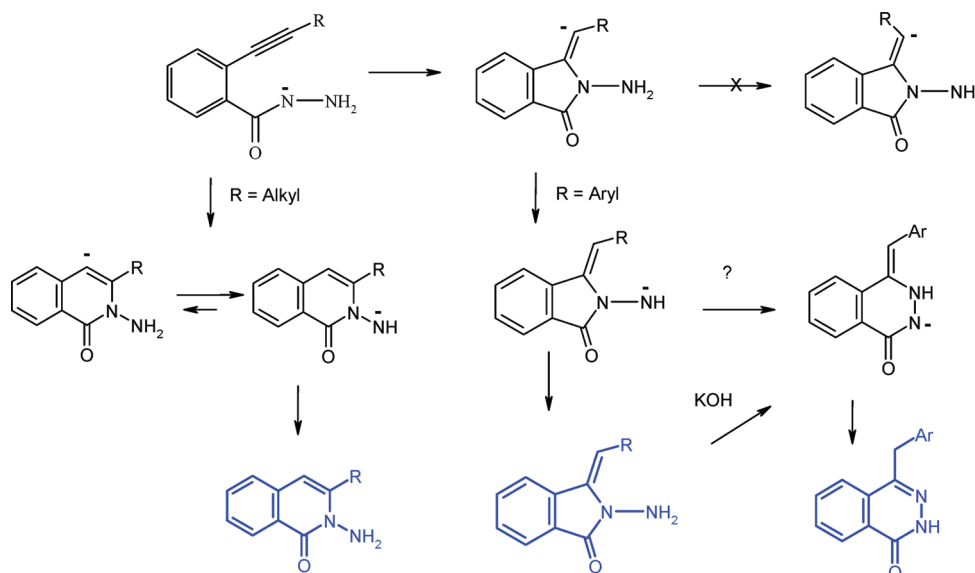
(41) (a) Muller, N.; Mulliken, R. S. *J. Am. Chem. Soc.* **1958**, *80*, 3489. For more recent examples, see: (b) Stability of  $\alpha$ -sulfonyl carbanions: Raabe, G.; Gais, H. J.; Fleischhauer, J. *J. Am. Chem. Soc.* **1996**, *118*, 4622. (c) Carbocations: Rauk, A.; Sorensen, T. S.; Maerker, C.; Carneiro, J. W. d. M.; Sieber, S.; Schleyer, P. v. R. *J. Am. Chem. Soc.* **1996**, *118*, 3761. (d) Kirchen, R. P.; Ranganayakulu, K.; Sorensen, T. S. *J. Am. Chem. Soc.* **1987**, *109*, 7811.

(42) Keith, B.; Khalaf, D.; Ghadir, F. J. *Chem. Soc., Perkin Trans.* **1990**, 1333.

SCHEME 10. Relative Stabilities in the Pairs of Stereoisomeric Cyclization Products at the B3LYP/6-31+G\*\* Level



Energies are given in kcal/mol; data for R = Ph are in parentheses.

SCHEME 11. Summary of accessible reaction pathways with the most likely intermediates for the anionic transformations of hydrazides of *o*-ethynyl substituted benzoic acids

interaction, which facilitates cyclization of the *Z*-isomer. Although the competing  $n_{C-} \rightarrow \sigma^*_{C-C}$  interaction with another vicinal antibonding orbital selectively stabilizes the opposite *E*-isomer, the latter interaction is weaker because of the weaker acceptor ability of  $\sigma^*_{C-C}$  orbitals in comparison with that of  $\sigma^*_{C-N}$  orbitals<sup>34d</sup> (Table 5).

The last remaining question is why the *E*-product is more stable despite the less favorable pattern of vicinal hyperconjugative interactions. The effect responsible for this switch in the relative stability has to develop relatively late along the reaction coordinate (after the transition state is passed) in order to explain the reversal of relative stability of the TS and products for the two stereoisomers. NBO analysis answers this question by detecting an intramolecular H-bonding interaction between the anionic carbon and an N–H bond of the exocyclic  $NH_2$  group. This interaction only fully develops at the late reaction stage in the *E*-conformer of the 5-*exo*-product (when the

anionic center and the N–H bond are brought closer in the cyclization step) and thus is not capable of influencing the *E*-transition state and perturbing kinetic competition between the two isomers. Since we do not observe formation of the more stable *E*-isomer, external protonation of the cyclic carbanions should be faster than conversion between the two stereoisomers. Taking into account that this reaction is carried out in ethanol as a solvent, this scenario is plausible.

### Conclusion

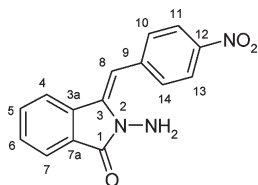
In summary, cyclizations of hydrazides of *o*-acetylenyl benzoic acids under basic conditions can be directed along three alternative paths depending on the external factors and the nature of substituents at the acetylenic moiety. Alkyl substituents at the alkyne terminus favor the 6-*endo*-dig closure whereas aryl groups greatly facilitate the alternative 5-*exo*-dig path. Synthetic utility of these processes is amplified by rearrangement of the initial 5-*exo*-dig cyclization

products into diazinone products of a formal 6-exo-dig cyclization via the less reactive external nitrogen participation. The latter process proceeds in an indirect way, through a sequence of nucleophilic attack, ring-opening, and recyclization which is negotiated through several proton shifts, ultimately leading to the most stable of tautomeric anions as a thermodynamic sink. The most likely reaction intermediates identified by the DFT analysis of potential energy surfaces for the competing rearrangements are summarized in Scheme 11. Trends discovered in this work allow selective transformation of a common precursor into benzopyrrolidones, benzopyridazines, or benzodiazinones—three promising biologically active classes of annealed heterocycles.

Finally, NBO analysis reveals that stereoelectronic hyperconjugative  $\sigma_{C-N} \rightarrow \sigma^*_{C-N}$  interactions efficiently control stereoselectivity of 5-exo-dig cyclization providing a kinetically favorable pathway to the thermodynamically unfavorable *Z*-isomer. Intramolecular H-bonding selectively stabilizes the *E*-isomer of the product but develops at the later reaction stage, after the TS.

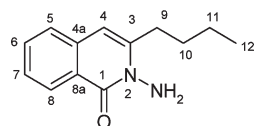
## Experimental Section

**(*Z*)-*N*-Amino-3-(4-nitrobenzylidene)isoindolin-1-one, 3c.** A mixture of 2.8 mmol of methyl ethynylbenzoate (**1c**)<sup>42</sup> and 4.2 mmol of 80%  $\text{NH}_2\text{NH}_2 \cdot \text{H}_2\text{O}$  were refluxed in 5 mL of ethanol for 7 h until full disappearance of the ester (TLC monitoring,  $\text{CH}_2\text{Cl}_2$ , EtOAc).



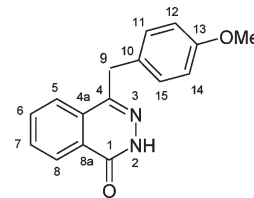
The reaction mixture was cooled and the precipitate was filtered off. Recrystallization from EtOH afforded compound **3c** (90%), mp 246–246.5 °C (from  $\text{C}_2\text{H}_5\text{OH}$ ): IR  $\nu/\text{cm}^{-1}$  1716 (C=O); HRMS, found  $m/z$  281.0802  $[\text{M}]^+$ ;  $\text{C}_{15}\text{H}_{11}\text{N}_3\text{O}_3$  calcd  $M = 281.0800$ ;  $^1\text{H}$  NMR ( $\text{CDCl}_3$ , 400.13 MHz)  $\delta$  4.31 (2H, s,  $\text{NH}_2$ ), 7.02 (1H, s, =CH), 7.39–7.48 (3H, m, H-4,5,6), 7.66 (2H, d, H-10, 14,  $J = 8.4$  Hz), 7.86 (1H, d, H-3,  $J = 7.6$  Hz), 8.29 (2H, d, H-11, H-13,  $J = 8.4$  Hz);  $^{13}\text{C}$  NMR  $\delta$  108.9 (C-8), 122.5 (C-4), 123.3 (C-7), 123.7 (C-10,14), 128.4 (C-3), 129.8 (C-6), 129.9 (C-11, C-13), 130.1 (C-5), 132.3 (C-3a), 137.4 (C-7a), 142.3 (C-9), 146.6 (C-12), 165.1 (C-1). Anal. Calcd for  $\text{C}_{15}\text{H}_{11}\text{N}_3\text{O}_3$ : C 64.05; H 3.94; N 14. Found: C 63.89; H 3.61; N 14.99.

***N*-Amino-3-butylisoquinolin-1-one, 5d.** A mixture of 40 mg (1.9 mmol) hydrazide **4d** and 10 mg (1.9 mmol) of KOH was refluxed in 5 mL of EtOH until full disappearance of the hydrazide (2 h, TLC control, EtOAc).



The reaction mixture was dried in vacuum, redissolved in benzene, and filtered through  $\text{Al}_2\text{O}_3$  (2.5 × 2 cm). After removal of benzene under vacuum, the product was crystallized from EtOH to afford 30 mg (75%) of **5d**: mp 75–76 °C (from EtOH); IR  $\nu/\text{cm}^{-1}$  1645 (C=O); HRMS, found  $m/z$  216.1254  $[\text{M}]^+$ ;  $\text{C}_{13}\text{H}_{16}\text{N}_2\text{O}$  calcd  $M = 216.1257$ ;  $^1\text{H}$  NMR ( $\text{CDCl}_3$ , 400.13 MHz)  $\delta$  0.96 (3H, t, Me,  $J = 7.2$  Hz), 1.43–1.76 (4H, m, H-10, H-11), 2.83 (2H, t, H-9,  $J = 7.6$  Hz), 4.95 (2H, s,  $\text{NH}_2$ ), 6.33 (1H, s, =CH), 7.46–7.60 (3H, m, H-5, H-6, H-7), 8.34 (1H, d, H-8,  $J = 8$  Hz);  $^{13}\text{C}$  NMR  $\delta$  13.7 (C-13), 22.2 (C-12), 30.4 (C-11), 32.0 (C-10), 103.7 (C-4), 123.3 (C-3), 125.2 (C-6), 125.5 (C-7), 127.3 (C-5), 131.9 (C-8), 136.2 (C-5a), 144.6 (C-8a), 162.2 (C-1). Anal. Calcd for  $\text{C}_{13}\text{H}_{16}\text{N}_2\text{O}$ : C 72.19; H 7.46; N 12.95. Found: C 72.12; H 7.46; N 12.63.

**4-(4-Methoxybenzyl)phthalazin-1(2H)-one, 6a.** A mixture of 2 mmol of isoindolinone **3a** and 2 mmol of KOH was refluxed in 5 mL of EtOH (TLC control, EtOAc) for 2 h.



The reaction mixture was dried under vacuum, redissolved in benzene, and filtered through  $\text{Al}_2\text{O}_3$  (2.5 × 2 cm). After removal of benzene under vacuum, the product was crystallized from EtOH. Compound **6a** (3 h, 70%): mp 193.5–194.5 °C (from  $\text{C}_2\text{H}_5\text{OH}$ ); IR  $\nu/\text{cm}^{-1}$  1665 (C=O); HRMS, found  $m/z$  266.1052  $[\text{M}]^+$ ;  $\text{C}_{16}\text{H}_{14}\text{N}_2\text{O}_2$  calcd  $M = 266.1050$ ;  $^1\text{H}$  NMR ( $\text{CDCl}_3$ , 300.13 MHz)  $\delta$  3.74 (3H, s,  $\text{OCH}_3$ ), 4.22 (2H, s,  $\text{CH}_2$ ), 6.80 (2H, d, H-12, H-14,  $J = 8.4$  Hz), 7.17 (2H, d, H-11, H-15,  $J = 8.4$  Hz), 7.71–7.76 (3H, m, H-5, H-6, H-7), 8.45 (1H, d, H-8,  $J = 9.6$  Hz), 10.58 (1H, s, NH);  $^{13}\text{C}$  NMR  $\delta$  37.9 (C-9), 55.1 (C-OMe), 114.0 (C-12, C-14), 122.9 (C-8a), 125.3 (C-5), 126.8 (C-8), 128.2 (C-10), 129.3 (C-11, C-15), 129.6 (C-4a), 131.1 (C-7), 133.3 (C-6), 146.5 (C-4), 158.2 (C-13), 160.4 (C-1). Anal. Calcd for  $\text{C}_{16}\text{H}_{14}\text{N}_2\text{O}_2$ : C 72.16; H 5.30; N 10.52. Found: C 72.25; H 5.27; N 10.58.

**Acknowledgment.** This work was supported by a grant from RFBR 07-03-00048-a, an Interdisciplinary grant from SB of the Russian Academy of Sciences No. 93 (2009-2011), an Intergrational grant from the Russian Academy of Sciences 5.9.3. (2009-2011), and the Chemical Service Center of SB RAS. I.A. is grateful to the National Science Foundation (CHE-0848686) and to the donors of Petroleum Research Fund, administered by the American Chemical Society (Award no. 47590-AC4) for partial support of his research at FSU.

**Supporting Information Available:** Full experimental details, NMR assignments, geometries and energies of calculated intermediates, and full reference 25. This material is available free of charge via the Internet at <http://pubs.acs.org>.